Overexpression of *C-sis* inhibits H$_2$O$_2$-induced Buffalo rat liver cell apoptosis *in vitro* and alleviates liver injury in a rat model of fulminant hepatic failure

HAO DING and ZHILI WEN

Department of Gastroenterology, The Second Affiliated Hospital of Nanchang University,
Nanchang, Jiangxi 330006, P.R. China

Abstract. The present study aimed to investigate the role of the *C-sis* gene in the apoptosis of hepatocytes *in vitro* and in the liver function of a rat model of fulminant hepatic failure (FHF). Buffalo rat liver (BRL) cells were treated with hydrogen peroxide (H$_2$O$_2$) to induce apoptosis and then transfected with a *C-sis* overexpression vector. A rat model of FHF was established, and *C-sis* was overexpressed. The mRNA and protein expression of *C-sis* were examined using reverse transcription-polymerase chain reaction and western blot analyses, respectively. Cell viability was assessed by CCK8, and a TUNEL assay was used to examine cell apoptosis. Flow cytometry was used for cell cycle detection. Hematoxylin and eosin staining was used for histological examination. The levels of alanine transaminase (ALT) and aspartate transaminase (AST) were also examined in the rats. The results showed that *C-sis* was successfully overexpressed in the cells and rat model. Compared with H$_2$O$_2$-treated BRL cells, the overexpression of *C-sis* significantly inhibited cell apoptosis, promoted cell viability, and decreased the expression of cleaved caspase-3. Similar results were observed in the FHF rats treated with the *C-sis* overexpression plasmid, compared with those treated with empty plasmids. In addition, in the FHF rats overexpressing *C-sis*, histological examination showed that liver injury was alleviated, the levels of ALT and AST were significantly decreased, and mortality rate was significantly decreased, compared with those observed in the rats treated with empty plasmids. In conclusion, the overexpression of *C-sis* inhibited the H$_2$O$_2$-induced apoptosis of BRL cells *in vitro*, and alleviated liver injury, improved liver function, and decreased mortality rates in rat models of FHF.

Correspondence to: Dr Zhili Wen, Department of Gastroenterology, The Second Affiliated Hospital of Nanchang University, 1 Minde Road, Nanchang, Jiangxi 330006, P.R. China
E-mail: zhili_ladh@163.com

Introduction

Fulminant hepatic failure (FHF), which is characterized by extensive hepatocyte necrosis (1), is a clinical syndrome that results from the severe impairment of liver function induced by drugs, toxins or viral hepatitis (2). Even in developed countries, the mortality rate of patients with FHF is as high as 50-90% without liver transplantation (3). However, patients with FHF usually suffer multiple organ failure, which prevents liver transplantation (4). In addition, due to donor liver shortages, high costs, complications, and the risk of organ rejection, the application of liver transplantation is limited (5). Biochemical and pathological studies have suggested that hepatocyte apoptosis is important in the development of FHF, resulting in substantial hepatocyte loss when the rate and extent of hepatocellular apoptosis are not adequately compensated by regenerative activity (5).

Under normal physiological conditions, proto-oncogenes are involved in the maintenance of tissue homeostasis (6). Proto-oncogene activation has been used to repair cardiac ischemia injury (7). The proto-oncogene *C-sis* encodes the B chain of platelet-derived growth factor (PDGF-B) (8). PDGF is a potent mitogen, which is released from activated hepatocytes and hepatic stellate cells (HSCs), which are involved in liver repair (9-11). At the cellular level, PDGF is one of the most well characterized fibrogenic and proliferative cytokines for HSCs. In addition, hepatic injury is associated with the upregulation of autocrine PDGF and PDGF receptor (10,12). Hao *et al* (13) demonstrated that the neutralization of PDGF-B suppressed the proliferation and activation of HSCs in the fibrotic mouse liver. PDGF-B may exist as a homodimer (PDGF-BB) or as a heterodimer with chain A (PDGF-AB). PDGF-BB serum levels are positively associated with survival rates among patients with FHF (14), indicating its potential role in the progression of FHF. PDGF-BB is the main stimulus for the proliferation of mesenchymal cells and is secreted by several cells residing in or passing through the liver (15). Hirota *et al* (16) reported that the overexpression of PDGF-BB resulted in airway hyper-responsiveness, decreased lung compliance, increased airway smooth muscle cell numbers, positive proliferating cell nuclear antigen-stained airway smooth muscle cells, and a reduction in genes encoding contractile proteins. Additionally,

PDGF-BB induces the proliferation of HSCs (12,17-23) and is also essential in the progression of liver fibrosis (23,24). Therefore, it was hypothesized that *C-sis* may be involved in the repair of liver injury in FHF by regulating hepatocellular apoptosis.

To validate the above hypothesis *in vitro* and *in vivo*, respectively, Buffalo rat liver (BRL) cells were treated with hydrogen peroxide (H_2O_2) to induce apoptosis or were transfected with a *C-sis* overexpression vector. A rat model of FHF was established, and *C-sis* was overexpressed. Cell viability and apoptosis were assessed. The results showed that the overexpression of *C-sis* inhibited the H_2O_2-induced apoptosis of BRL cells *in vitro*, and alleviated liver injury and decreased mortality rates in the FHF rats.

Materials and methods

Plasmid construction. The full-length cDNA encoding rat *C-sis* (GenBank™ accession no. NM24628) was generated by reverse transcription-polymerase chain reaction (RT-PCR) from the liver tissues of Sprague-Dawley rats, using the following primers: Forward, 5'-CGCGAATTCATGAATCGC TGCTGGGC-3' (the *Eco*RI site is underlined) and reverse, 5'-CCCTCTAGACTAGGCTCCAAGGATCTC-3' (the *Xba*I site is underlined). The PCR products were digested and cloned into the mammalian expression vector pcDNA3.1 (Invitrogen; Thermo Fisher Scientific, Inc., Waltham, MA, USA). The plasmids were purified using the AxyPrep DNA Gel Recovery kit (Axygen Biotechnology Co., Ltd., Hangzhou, China).

Cell culture, transfection and H_2O_2 treatment. The BRL cells (Shanghai Cell Bank, Chinese Academy of Sciences, Shanghai, China) were cultured in DMEM containing 10% FBS (Gibco; Thermo Fisher Scientific, Inc.) in a humidified incubator at 37˚C under 5% CO_2. Cells in the logarithmic phase were digested with 0.25% trypsin and 0.02% EDTA, and then centrifuged at 513 x g for 5 min at 37˚C. The cells ($8x10^4$ cells/well) were placed in an incubator under 5% CO_2 at 37˚C. Following complete attachment to the walls, 2 μg of plasmid and 4 μl of Lipo3000 (Invitrogen; Thermo Fisher Scientific, Inc.) were added. After 6-8 h, the medium was discarded and replaced with DMEM with or without the addition of 200 μM of H_2O_2 for 48 h. The groups used were as follows: Control (no H_2O_2), empty plasmid (no H_2O_2), *C-sis* plasmid (no H_2O_2), H_2O_2 group (no plasmid), empty plasmid+H_2O_2, and *C-sis* plasmid+H_2O_2.

Animals. Female Sprague-Dawley rats (n=100, age, 8-10 weeks, weight, 200±10 g) were purchased from Changzhou Cavens Laboratory Animal Co., Ltd. (Changzhou, China). The rats were housed one per cage in a room maintained at 24-25˚C on a 12-h light/dark cycle with free access to food and water. The present study was approved by the Animal Ethics Committee of the Second Affiliated Hospital of Nanchang University (Nanchang, China). All animal procedures were performed in strict accordance with the guidelines for the Care and Use of Laboratory Animals published by the US National Institutes of Health (NIH publication no. 85-23, revised 1996). Transfection of the target *C-sis* gene was performed using hydrodynamics-based transfection *in vivo*, as described previously (25,26).

FHF modeling and grouping. At 48 h post-transfection, 40 rats were randomized into four groups (n=10 in each group): Group A, normal control rats; group B, FHF and Ringer's solution (FHF+Ringer's solution injection group); group C, FHF and empty vector pcDNA3.1 (FHF+empty plasmid group); and group D, FHF and constructed plasmid pcDNA3.1/*C-sis* (FHF+C-sis plasmid group). FHF was induced through an intraperitoneal injection of 50 μg/kg of lipopolysaccharide (LPS) and 300 mg/kg of D-galactosamine (D-GalN) (27). At 8 h post-injection, the liver tissues and blood samples of the normal control group (n=10), the FHF+Ringer's solution injection group (n=9), the FHF+empty plasmid group (n=9), and the FHF+*C-sis* plasmid group (n=10) were collected. Another 40 rats were grouped as above (n=10 in each group) to evaluate the 24-h mortality.

C-sis mRNA. Total RNA was extracted using the Rapid Extraction kit for total RNA (Generay Biotech Co., Ltd., Shanghai, China). First-strand cDNA was synthesized from 2 μg of total RNA by using the TaqMan Reverse Transcription Reagents kit (Thermo Fisher Scientific, Inc.) with oligo(dT)[16] primer. The RNA-primer mix was heated at 42˚C for 5 min, and then incubated on ice for at least 1 min The PCR primers were designed using Primer Premier 5.0 software (Premier Biosoft International, Palo Alto, CA, USA) based on previously reported sequences (GenBank™ accession no. NM_24628 for *C-sis*, NM_81822 for β-actin). The primers were as follows: *C-sis*, forward, 5'-ATGACCCGAGCACATTCTGG-3' and reverse, 5'-ACACCTCTGTACGCGTCTTG-3'; and β-actin, forward, 5'-CCCATCTATGAGGGTTACGC-3' and reverse, 5'-TTTAATGTCACGCACGATTTC-3'. The PCR analysis was performed with 500 ng of cDNA, 1 μl of each primer, 10 μl of 2X SuperReal premix plus, and ddH_2O to achieve a final volume of 20 μl. The conditions were as follows: i) 95.0˚C for 15 min; ii) 40 cycles at 95.0˚C for 10 sec, 60.0˚C for 20 sec, and 72.0˚C for 20 sec. The results were calculated and analyzed using quantitative fluorescence PCR analysis software (BIO-RAD CFX Manager version 3.0; Bio-Rad Laboratories, Inc., Hercules, CA, USA).

Western blot analysis. Total proteins were extracted using a total protein extraction kit. The protein concentrations were determined using BCA protein assay kit (Beyotime Institute of Biotechnology, Shanghai, China). The proteins (100 μg, 7 μg/μl) were separated by 10% denaturing SDS-polyacrylamide gel electrophoresis and transferred onto a polyvinylidene difluoride membrane. The membrane was blocked with 5% non-fat dry milk for 1 h at room temperature, washed, and blotted with primary antibodies against *C-sis* (cat. no. ab78409; 1:400), cleaved poly (ADP-ribose) polymerase 1 (PARP1; cat. no. ab32064; 1:1,000), cleaved caspase-3 (cat. no. ab2302; 1:1,000), B-cell lymphoma 2 (Bcl-2; cat. no. ab196495; 1:1,000), Bcl-2-associated X protein (Bax; cat. no. ab32503; 1:1,000) (all from Abcam, Cambridge, MA, USA), or GAPDH (cat. no. AP0063; 1:400; Bioworld Technology, Inc., Louis Park, MN, USA), and incubated overnight at 4˚C. This was followed by incubation with a horseradish peroxidase-conjugated goat anti-rabbit immunoglobulin G (cat. no. A50-106P; 1:1,000; Origene Technologies, Inc, Beijing, China) at room temperature for 1 h. The bands were quantified using Quantity One

4.62 software (Bio-Rad Laboratories, Inc.). GAPDH was used as an internal control.

Histological examination. The liver tissues were fixed in 10% formaldehyde solution for 30 min at room temperature, paraffin-embedded, sectioned at 4-μm, and stained using hematoxylin and eosin at room temperature for 10 min under an Olympus BH-2 light microscope (Olympus Corporation, Tokyo, Japan).

Cell viability. Cell viability was assessed using the CCK8 assay. The cells (100 μl; 5,000 cells/well) were added to a 96-well plate. The plate was incubated for 48 h at 37°C under 5% CO_2. The medium was then discarded and replaced with fresh medium containing 10 μl of CCK8 solution (Beyotime Institute of Biotechnology, Shanghai, China). Blank control wells received 0.9% saline. The plates were incubated at 37°C for 1 h in the dark. The optical density was measured at 450 nm.

TUNEL assay. Cell apoptosis was detected using a commercial TUNEL assay (cat. no. 11684817910; Roche Applied Science, Penzberg, Germany), in strict accordance with the manufacturer's protocol. The slides were counterstained using hematoxylin at room temperature for 1 min, and sealed with neutral gum.

Cell apoptosis. A Cell Apoptosis kit (UNOCI Biological Technology Co., Ltd., Hangzhou, China) was used to detect cell apoptosis, in strict accordance with the manufacturer's protocol. A flow cytometer (ACCURI C6; BD Biosciences, Franklin Lake, NJ, USA) was used to detect apoptotic cells. The data was analyzed using FlowJo software version 10.0.5 for Microsoft (FlowJo LLC, Ashland, OR, USA).

Cell cycle analysis. A Cell Cycle Analysis kit (Beyotime Institute of Biotechnology) was used to measure cell cycle data. Briefly, the cells were collected by centrifugation at 513 x g for 15 min at 37°C, washed twice with 4°C PBS, and fixed with 75% cold ethanol at 4°C for 24 h. The cells were collected by centrifugation at 513 x g for 5 min at 37°C, dried, and washed twice with PBS. Subsequently, 1 ml of Reagent A was added; the tube was then mixed well for 5-10 sec and incubated for 30 h. Flow cytometry (ACCURI C6; BD Biosciences) was used to measure cell cycle data.

Immunohistochemistry. The liver tissues were fixed with 4% paraformaldehyde solution at room temperature for 30 min, paraffin-embedded, sectioned at 4-μm, and dewaxed. Endogenous peroxidase was blocked and inactivated, and the sections were blotted overnight at 4°C with a primary antibody against caspase-3 (cat. no. ab2302; 1:100; Abcam), followed by incubation with the biotinylated rabbit secondary antibody (cat. no. BA1100; 1:375; Vector Laboratories, Inc., Burlingame, CA, USA) at 37°C for 1 h. Finally, the sections were stained with DAB and then counterstained with hematoxylin at room temperature for 1 min. Three different fields were selected from each section under an Olympus BH-2 light microscope (Olympus Corporation; magnification, x200). The intensity of the expression and the positivity rate were measured. The
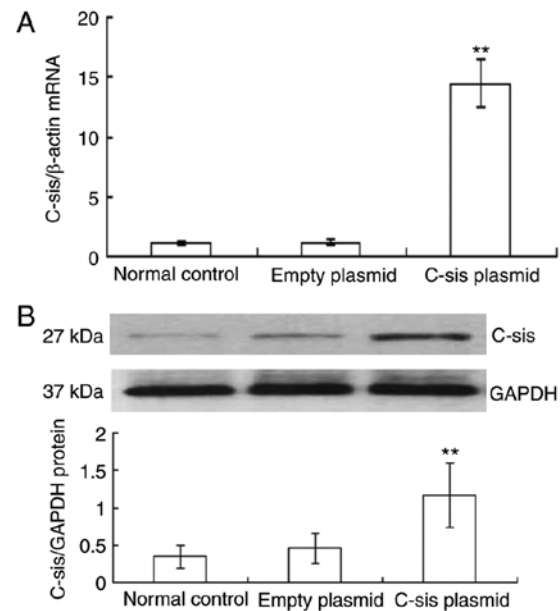

Figure 1. Overexpression of *C-sis* in BRL cells. (A) mRNA expression of *C-sis* detected by fluorescence quantitative PCR at 48 h post-transfection. (B) Protein expression of *C-sis* detected by fluorescence quantitative PCR at 48 h post-transfection. **P<0.01 vs. empty plasmid group. BRL, Buffalo rat liver; PCR, polymerase chain reaction.

expression score was calculated as the staining intensity multiplied by the percentage of positive cells, as previously described (28).

Alanine transaminase (ALT) and aspartate transaminase (AST) measurement. An ALT detection kit (Nanjing Jiancheng Bioengineering Institute, cat. no. C009-2, batch no. 20141105) and an AST detection kit (Nanjing Jiancheng Bioengineering Institute, cat. no. C0010-2, batch no. 20141104) were used in strict accordance with the manufacturer's protocol.

Statistical analysis. Data are presented as the mean ± standard deviation and were analyzed using one-way analysis of variance followed by the least significant difference test. Statistical analysis was performed using SPSS 13.0 (SPSS, Inc., Chicago, IL, USA). Each experiment was repeated three times. P<0.05 was considered to indicate a statistically significant difference.

Results

Overexpression of C-sis in BRL cells. Reactive oxygen species are crucial in FHF and acute hepatic failure (29). The present study used H_2O_2, which is known to induce apoptosis in mouse primary cultured hepatocytes (30), to cause oxidative stress and thereby induce apoptosis of BRL cells. Compared with the control and empty plasmid groups, the mRNA expression of *C-sis* in the *C-sis* plasmid group was significantly increased at 48 h post-transfection (P<0.01; Fig. 1A). Similarly, the protein expression of *C-sis* in the *C-sis* plasmid group at 48 h post-transfection was significantly increased when compared with the control and the empty plasmid groups (P<0.01; Fig. 1B). These results showed that *C-sis* was successfully overexpressed in the BRL cells.
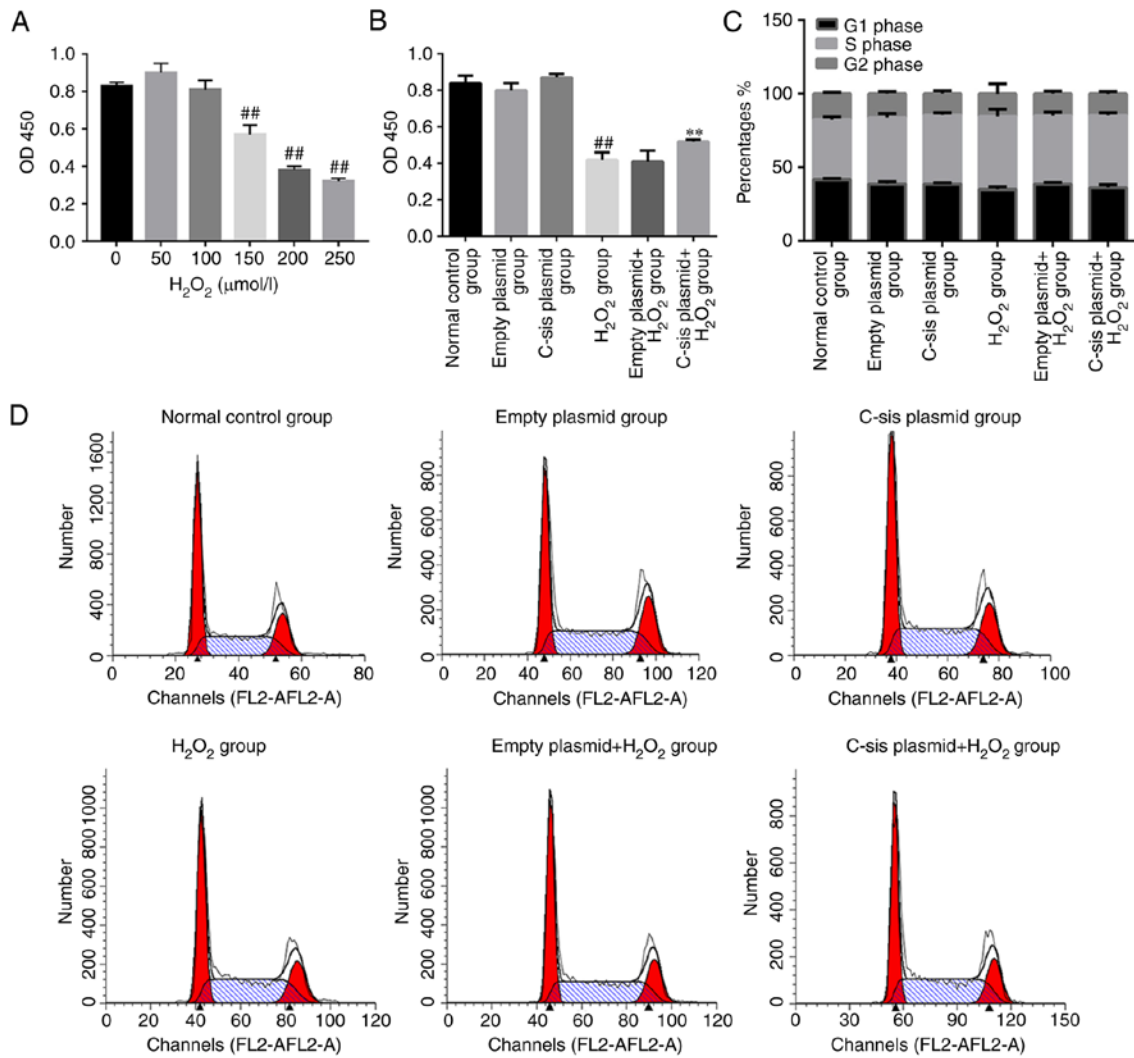
Figure 2. Cell viability and cell cycle data in each group. (A) A CCK8 assay was performed to detect the viability of BRL cells treated with increasing concentrations of H_2O_2. (B) A CCK8 assay was performed to detect the viability of BRL cells with the indicated treatment in each group. ##P<0.01 vs. normal control group; **P<0.01 vs. empty plasmid+H_2O_2 group. (C) Representative flow cytometry data for BRL cell cycle. (D) BRL cell cycle data among the groups. BRL, Buffalo rat liver; H_2O_2, hydrogen peroxide.

Cell viability and cell cycle analysis in each group. Reactive oxygen species are crucial in FHF and acute hepatic failure (29). H_2O_2 treatment led to a significant decrease in cell viability when the concentration of H_2O_2 reached 150 μmol/l (Fig. 2A). As shown in Fig. 2B, the cell viability in the H_2O_2 group was significantly decreased compared with that in the control group (P<0.01). Compared with the empty plasmid+H_2O_2 group, the cell viability in the *C-sis* plasmid+H_2O_2 group was significantly increased (P<0.01). Cell cycle was assessed by flow cytometry and the results demonstrated no significant differences in cell cycle among the groups (Fig. 2C and D).

Cell apoptosis in each group. Four populations of cells were detected using flow cytometry: Q1-UL (necrotic cells and debris), Q1-UR (late stage apoptotic cells and necrotic cells), Q1-LL (normal cells), and Q1-LR (apoptotic cells at the early stage, as detected by CCK8). The sum of Q1-UR and Q1-LR was considered the apoptotic rate. Compared with the normal control group, cell apoptosis in the H_2O_2 group was significantly increased (P<0.01). Compared with the empty

plasmid+H_2O_2 group, cell apoptosis of the *C-sis* plasmid+H_2O_2 group was significantly decreased (P<0.01; Fig. 3A and B). The results of the TUNEL assay were consistent with the flow cytometry results (Fig. 3C and D).

In addition, as shown in Fig. 3E, the protein expression levels of the pro-apoptotic proteins, cleaved caspase-3, cleaved PARP1 and Bax, were significantly increased in the H_2O_2 group, compared with those in the normal control group (P<0.01). Compared with the empty plasmid+H_2O_2 group, the expression levels of cleaved caspase-3, cleaved PARP1 and Bax were significantly decreased in the *C-sis* plasmid+H_2O_2 group (P<0.01). However, the anti-apoptotic protein Bcl-2 showed the opposite protein expression pattern compared with the three pro-apoptotic proteins.

Overexpression of C-sis in the FHF rat models. There was a significant increase in the mRNA expression of *C-sis* in the *C-sis* plasmid group compared with the normal control and empty plasmid groups (P<0.01; Fig. 4A), and there was a significant increase in the protein expression of *C-sis* in the *C-sis* plasmid group compared with the normal control and
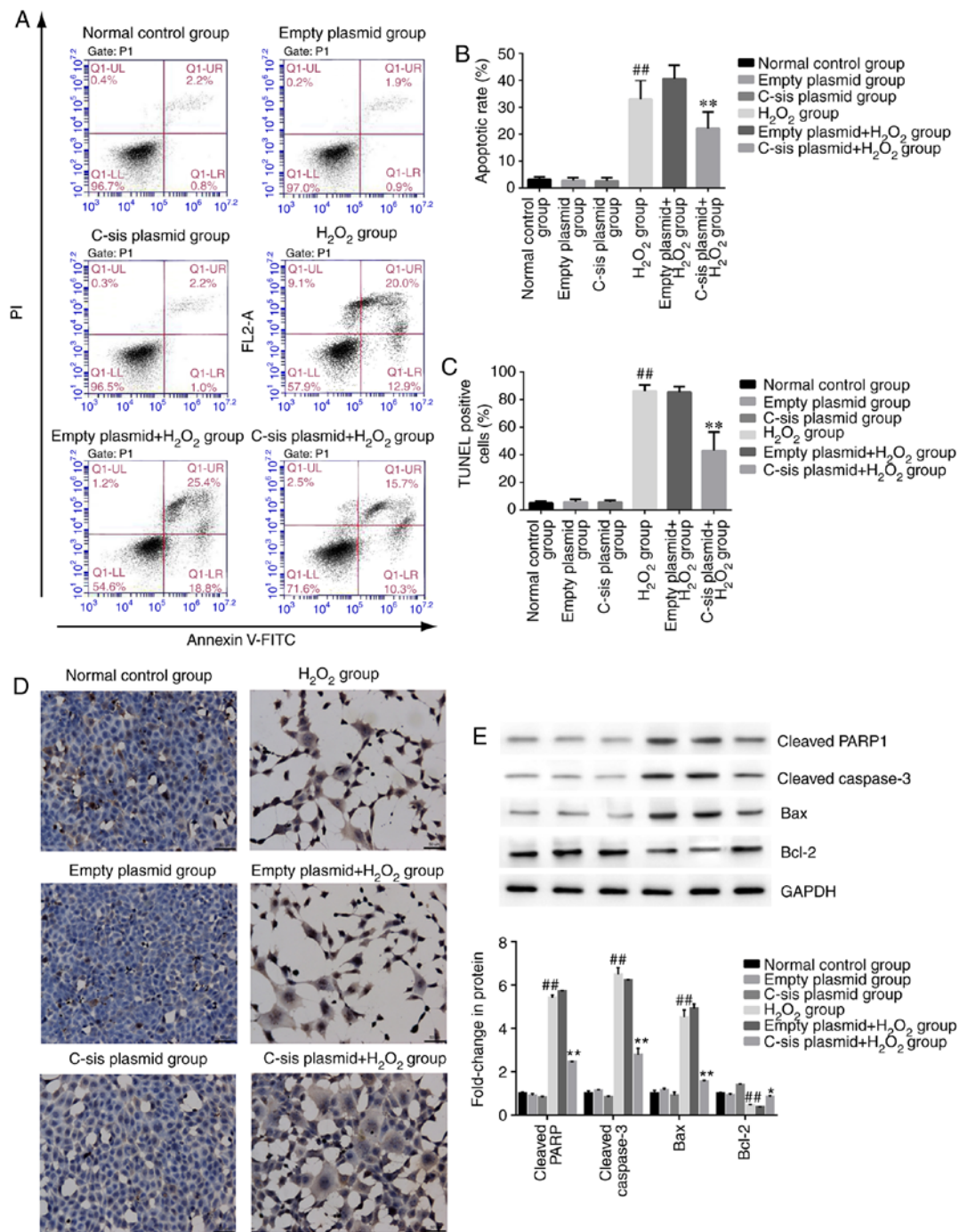
Figure 3. Cell apoptosis in each group. (A) Representative results of BRL cell apoptosis, measured by flow cytometry. (B) BRL cell apoptosis detected by flow cytometry. The results are presented as the mean ± standard deviation calculated from five replicates. ##P<0.01 vs. normal control group; **P<0.01 vs. empty plasmid+H$_2$O$_2$ group. (C) Detection of BRL cell apoptosis using the TUNEL assay. The results are presented as the mean ± standard deviation calculated from four replicates. ##P<0.01 vs. normal control group; **P<0.01 vs. empty plasmid+H$_2$O$_2$ group. (D) Representative images of sections stained with TUNEL. Magnificatiion, x200. (E) Western blot analysis of cleaved PARP1, cleaved caspase-3, Bax, and Bcl-2 in BRL cells. Values are presented as the mean ± standard deviation calculated from five replicates. ##P<0.01. vs. normal control group. *P<0.05 vs. empty plasmid+H$_2$O$_2$ group. BRL, Buffalo rat liver; H$_2$O$_2$, hydrogen peroxide; PARP1, poly (ADP-ribose) polymerase 1; Bcl-2, B-cell lymphoma 2; Bax, Bcl-2-associated X protein.

empty plasmid groups (P<0.01; Fig. 4B). These results showed that *C-sis* was successfully overexpressed in the FHF rats.

Histological examination in each group. In the normal control group, the cellular structure of the liver tissue was normal, and the liver cells were tightly arranged. The nuclei were round, and the cells were without lesions in the form of lipid droplets, inflammation or necrosis. The lobular structure was normal,

and hepatocytes and sinusoidal cells were radially arranged around the central vein (Fig. 5A). In the FHF+Ringer's solution injection group, the infiltration of inflammatory cells, mainly neutrophils, was observed. Scattered cell apoptosis was observed inside the liver of eight rats, and extensive necrosis was observed in one rat. The organizational structure of the liver had disappeared, and blood stasis was observed within the sinusoid (Fig. 5A). In the FHF+empty plasmid group, the
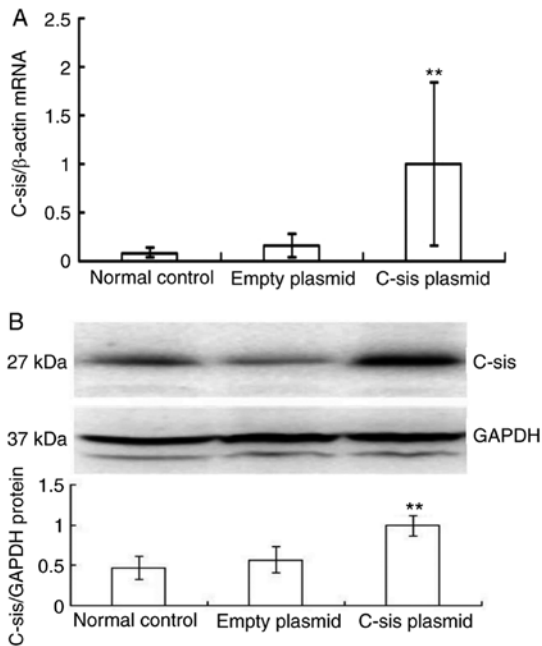
Figure 4. Overexpression of *C-sis* in the fulminant hepatic failure rat model. (A) mRNA expression of *C-sis* in the rat liver as measured by fluorescence quantitative polymerase chain reaction analysis. **P<0.01 vs. normal control and empty plasmid groups. (B) Protein expression of *C-sis* in rat liver detected by western blot analysis (n=10 in each group). **P<0.01 vs. empty plasmid group.

infiltration of inflammatory cells, mainly neutrophils, was observed. Scattered cell apoptosis was observed in the liver of seven rats, whereas extensive necrosis was observed in two rats. Marked blood stasis was found in the sinusoid (Fig. 5A). In the FHF+*C-sis* plasmid group, small focal inflammation with neutrophils was observed in the liver tissue. Cell apoptosis was observed in four rats, in which the nuclei were condensed. Cell structure was destroyed and extensive necrosis was present in one rat (Fig. 5A). Together, these results showed that the overexpression of *C-sis* alleviated liver injury.

Apoptosis in each group. Compared with the normal control group, there was a significant increase in cell apoptosis in the FHF+Ringer's solution injection group (P<0.01). Compared with the FHF+empty plasmid group, there was a significant decrease in cell apoptosis in the FHF+*C-sis* plasmid group (P<0.01; Fig. 5B and C). Compared with the normal control group, there was a significant increase in cleaved caspase-3 in the FHF+Ringer's solution injection group (P<0.01). Compared with the FHF+empty plasmid group, there was a significant decrease in cleaved caspase-3 in the FHF+*C-sis* plasmid group (P<0.05; Fig. 5D and E).

Serum levels of ALT and AST in each group. Compared with the normal control group, the serum levels of ALT (P<0.01) and AST (P<0.05) in the FHF+Ringer's solution injection group were significantly increased. Compared with the FHF+empty plasmid group, the serum levels of ALT (P<0.01) and AST (P<0.05) in the FHF+*C-sis* plasmid group were significantly decreased (Fig. 6A and B).

Animal mortality rates in each group. Within the 24-h observation period, all rats in the normal control group

survived, whereas 70.0 and 80.0% of the rats died within 24 h in the FHF+Ringer's injection and FHF+empty plasmid groups, respectively. Transfection of cells with the *C-sis* gene effectively protected the animals from death induced by LPS/D-GalN, and only two of these rats (20.0%) died within the 24-h observation period (Table I).

Discussion

The present study aimed to investigate the role of the *C-sis* gene in the apoptosis of hepatocytes *in vitro* and in liver function in a rat model of FHF. The results showed that the overexpression of *C-sis* not only inhibited the H_2O_2-induced apoptosis of hepatocytes *in vitro* but also improved liver function and decreased mortality in the rat models of FHF. Previous studies have shown that FHF mainly involves hepatocyte apoptosis rather than necrosis (14,31-33). Therefore, the inhibition of hepatocyte apoptosis can assist in preventing hepatocyte necrosis.

Previous studies have shown that PDGF-BB is involved in the resistance against oxidative stress in vascular smooth muscle cells (34), neurons (35,36), the intestine (37), and liver (38). The results of the present study showed that the overexpression of *C-sis* inhibited H_2O_2-induced BRL cell apoptosis. However, no significant difference in cell cycle was observed among the groups. The possible reason for this may be that the *C-sis* gene can function only through cell apoptosis and exerts no effect on the cell cycle. The *in vivo* experiments showed that the overexpression of *C-sis* alleviated histological damage, improved liver function, and decreased mortality rate in the FHF rats. To a certain extent, these results are consistent with a previous study showing that low plasma levels of PDGF-BB were associated with poor prognosis in patients with FHF (14). Taken together, the results of the present study suggested that *C-sis* d cell viability and inhibited apoptosis, and promoted tissue repair. Therefore, it was hypothesized that *C-sis* may have a positive role in the repair of damaged liver tissue and in the treatment of FHF.

The basal function of *C-sis* is to promote the intracellular transduction of mitotic signals and promote cell proliferation (39,40). *C-sis* encodes PDGF-B, which is a potent mitogenic source that can stimulate the division and proliferation of mesenchymal cells, and has a positive role in promoting vascular regeneration and wound healing (41,42). PDGF-B can stimulate the healing of ulcers in diabetic rats (43). Novel technologies are being developed that focus on the slow release of PDGF-B from a membrane to accelerate wound healing in patients with diabetes (44). The loss of function caused by PDGF-B mutation can lead to primary familial cerebral calcification, resulting in neurodegenerative disease (45,46).

The present study also considered the problem of carcinogenesis that arises following the long-term presence of the proto-oncogene *C-sis*. The majority of current findings related to *C-sis* are focused on the fact that *C-sis* can promote cell growth and tissue repair, however, certain studies have focused on the occurrence and progression of tumors (20). This is the reason why *C-sis* was selected for the treatment of FHF in the present study rather than other proto-oncogenes. Second, the present study aimed to observe the efficacy of *C-sis* on
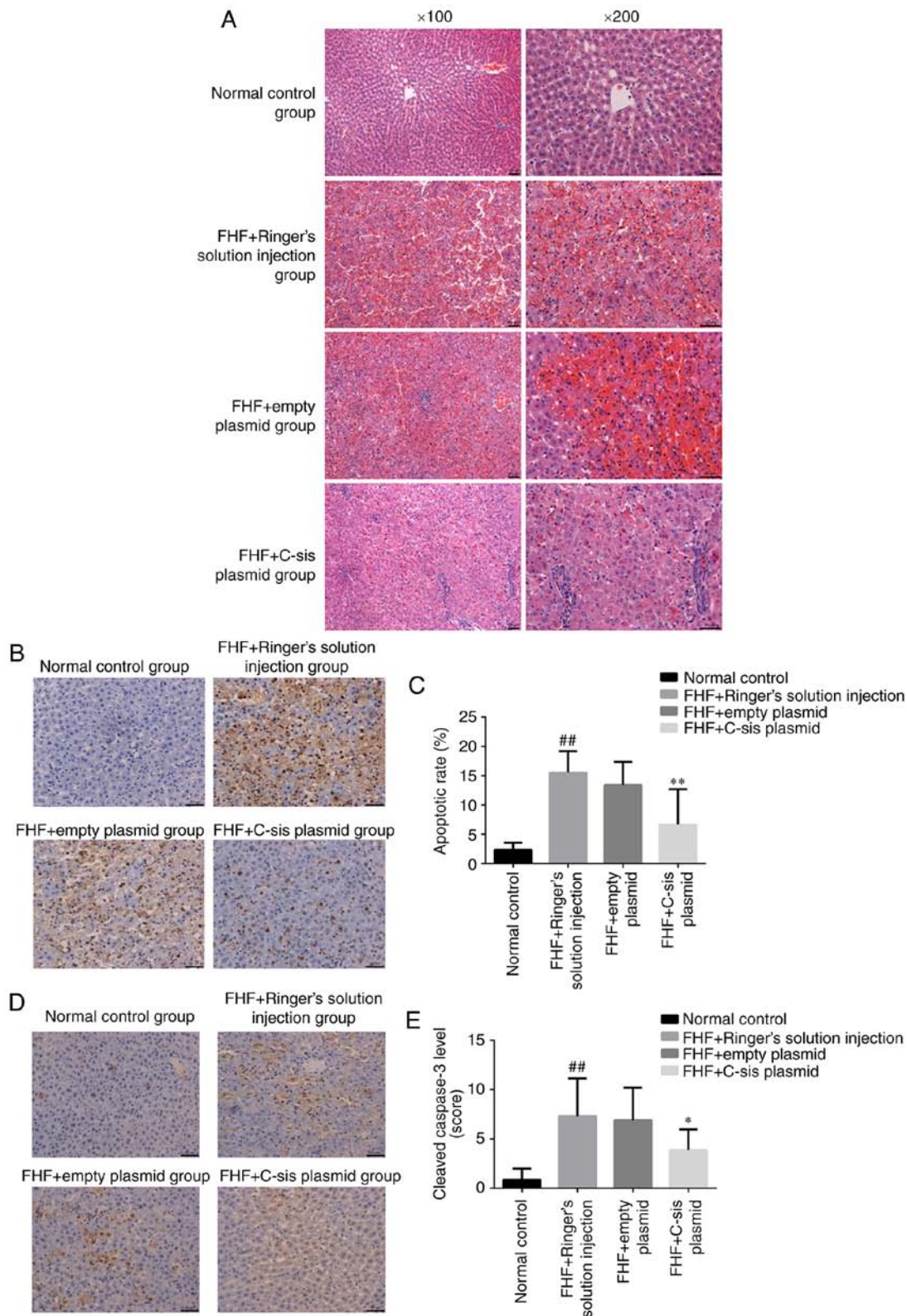
Figure 5. Apoptosis in each group. (A) Hematoxylin and eosin staining of liver sections of rats in the different groups. Magnification, x200. (B) Representative images of sections showing cell apoptosis in the liver of rats detected by TUNEL. Magnification, x200. (C) Cell apoptosis in the liver of rats detected by TUNEL. The results are presented as the mean ± standard deviation. ##P<0.01 vs. normal control group; **P<0.01 vs. FHF+empty plasmid group. (D) Representative sections showing the expression of caspase-3 in the liver tissue of rats by immunochemistry. Magnification, x200. (E) Expression of caspase-3 in the liver tissue of rats as shown by immunochemistry. The results are shown as the mean ± standard deviation. ##P<0.01 vs. normal control group; *P<0.05 vs. FHF+empty plasmid group. Normal control group (n=10), FHF+Ringer's solution injection group (n=9), FHF+empty plasmid group (n=9), and FHF+C-sis plasmid group (n=10). FHF, fulminant hepatic failure.

an acute life-threatening disease, FHF. Proto-oncogenes exist in the normal human body but are usually inactive. The

occurrence of cancer is a process that depends on numerous steps, and involves the activation of several proto-oncogenes

Table I. Mortality rate of the rats in the animal model of FHF.

Group	0 h	4 h	8 h	12 h	24 h	Mortality (%)
Normal control	0	0	0	0	0	0.00
FHF+Ringer's solution injection	0	0	3	2	2	70.00[a]
FHF+empty plasmid	0	0	3	3	2	80.00
FHF+*C-sis* plasmid	0	0	0	2	0	20.00[b]

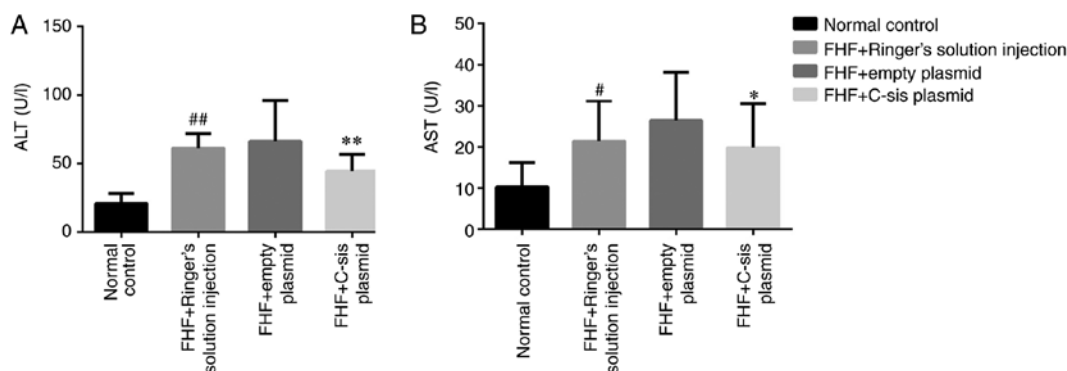[a]$P<0.01$ vs. normal control group; [b]$P<0.01$ vs. FHF+empty plasmid group. FHF, fulminant hepatic failure.

Figure 6. Serum ALT and AST levels in each group. Serum (A) ALT and (B) AST levels in each group. The results are presented as the mean ± standard deviation. ##$P<0.01$ (ALT) and #$P<0.05$ (AST) vs. normal control group; **$P<0.01$ (ALT) and *$P<0.05$ (AST) vs. FHF+empty plasmid group. Normal control group (n=10), FHF+Ringer's solution injection group (n=9), FHF+empty plasmid group (n=9), and FHF+*C-sis* plasmid group (n=10). ALT, alanine transaminase; AST, aspartate transaminase; FHF, fulminant hepatic failure.

and the inactivation of tumor suppressor genes; the activation of a single proto-oncogene may not cause cancer to arise. In addition, the inactivation of tumor suppressor genes is the main cause of cancer. Finally, previous studies performed experiments in which the proto-oncogene Pim-3 was used for the treatment of heart or liver failure; however, no tumor occurrence was observed (25,47).

H_2O_2 is a potent oxidant, and studies have shown that H_2O_2 can induce hepatocyte apoptosis (48,49). In the present study, LPS and D-GalN did not exert a significant effect on the proliferation of the BRL liver cell line (data not shown). Fas and ischemia-reperfusion can be separately used for the induction of mouse models of liver failure, whereas H_2O_2 is used to induce injury in cells (50,51). Therefore, in the present study, different methods had to be used to induce liver cell damage in the animals and in the cell line, which is a limitation of the study. Other limitations include the lack of comprehensive molecular analyses to determine the exact pathways involved in the response to the overexpression of *C-sis*, and the lack of investigation of the cytokines involved. In addition, only the short-term effects of the overexpression of *C-sis* were examined, although it is known that PDGF-BB can be involved in long-term liver fibrosis (52). These issues are to be examined in future investigations.

Increasing evidence suggests the novel involvement of the nucleolus in sensing cellular stress signals (53). Under stress conditions, the structure of the nucleolus is perturbed and certain nucleolar proteins, including ribosomal proteins, are released from the nucleolus to the nucleoplasm where they associate with Mouse Double Minute 2 (MDM2) to inhibit its

activity and stabilize p53 (53,54). Reactive oxygen species are crucial in FHF (55). The present study used H_2O_2 to induce oxidative stress in order to induce the apoptosis of BRL cells. Upon cell exposure to H_2O_2, redox changes in the nucleolar compartment are associated with activation of the ribosomal protein/MDM2/p53 pathway leading to apoptosis. In addition, previous data suggests that nuclear factor (NF)-κB is involved in apoptosis as part of the cell response to the nucleolar stress triggered by 5-fluorouracil (56). Inflammation is essential for the pathogenesis of FHF (55), and the NF-κB pathway has been shown to be key in the activation of the pro-inflammatory mechanism in FHF (55,57). These findings may assist in understanding the plausible molecular mechanisms underlying the role of *C-sis* in apoptosis.

In conclusion, the results of the present study showed that the overexpression of *C-sis* inhibited the H_2O_2-induced apoptosis of BRL cells *in vitro*, and alleviated liver injury, improved liver function and decreased mortality rate in rat model of FHF. These findings may assist in understanding the progression of FHF and may provide potential therapeutic approaches.

Acknowledgements

Availability of data and materials

The datasets used and/or analysed during the current study are available from the corresponding author on reasonable request.

Authors' contributions

HD and ZW conceived and designed the study. HD performed the experiments and wrote the paper. ZW reviewed and edited the manuscript. All authors read and approved the manuscript.

Ethics approval and consent to participate

The present study was approved by the Animal Ethics Committee of the Second Affiliated Hospital of Nanchang University. All animal procedures were performed in strict accordance with the guidelines for the Care and Use of Laboratory Animals published by the US National Institutes of Health (NIH publication no. 85-23, revised 1996).

Consent for publication

Not applicable.

Competing interests

The authors declare that they have no competing interests.

References

1. Moreau R: The pathogenesis of ACLF: The inflammatory response and immune function. Semin Liver Dis 36: 133-140, 2016.
2. Tuñón M, San-Miguel B, Crespo I, Jorquera F, Santamaría E, Alvarez M, Prieto J and González-Gallego J: Melatonin attenuates apoptotic liver damage in fulminant hepatic failure induced by the rabbit hemorrhagic disease virus. J Pineal Res 50: 38-45, 2011.
3. Hoofnagle JH, Carithers RL Jr, Shapiro C and Ascher N: Fulminant hepatic failure: Summary of a workshop. Hepatology 21: 240-252, 1995.
4. Campbell DA Jr, Ham JM, Mccurry KR, Lucey MR, Turcotte JG and Merion RM: Liver transplant for fulminant hepatic failure. Am Surg 57: 546-549, 1991.
5. Andrew SdMD and Parsia AVMD: Expanding the donor pool in liver transplantation: Extended criteria donors. Clin Liver Dis 2: 156-159, 2013.
6. Dunn S and Cowling VH: Myc and mRNA capping. Biochim Biophys Acta 1849: 501-505, 2015.
7. Landau E, Tirosh R, Pinson A, Banai S, Even-Ram S, Maoz M, Katzav S and Bar-Shavit R: Protection of thrombin receptor expression under hypoxia. J Biol Chem 275: 2281-2287, 2000.
8. Hellström M, Kalen M, Lindahl P, Abramsson A and Betsholtz C: Role of PDGF-B and PDGFR-beta in recruitment of vascular smooth muscle cells and pericytes during embryonic blood vessel formation in the mouse. Development 126: 3047-3055, 1999.
9. Zhao S, Zhang Z, Qian L, Lin Q, Zhang C, Shao J, Zhang F and Zheng S: Tetramethylpyrazine attenuates carbon tetrachloride-caused liver injury and fibrogenesis and reduces hepatic angiogenesis in rats. Biomed Pharmacother 86: 521-530, 2017.
10. Sun WY, Song Y, Hu SS, Wang QT, Wu HX, Chen JY and Wei W: Depletion of β-arrestin2 in hepatic stellate cells reduces cell proliferation via ERK pathway. J Cell Biochem 114: 1153-1162, 2013.
11. Wilhelm A, Aldridge V, Haldar D, Naylor AJ, Weston CJ, Hedegaard D, Garg A, Fear J, Reynolds GM, Croft AP, et al: CD248/endosialin critically regulates hepatic stellate cell proliferation during chronic liver injury via a PDGF-regulated mechanism. Gut 65: 1175-1185, 2016.
12. Kastanis GJ, Hernandez-Nazara Z, Nieto N, Rincón-Sanchez AR, Popratiloff A, Dominguez-Rosales JA, Lechuga CG and Rojkind M: The role of dystroglycan in PDGF-BB-dependent migration of activated hepatic stellate cells/myofibroblasts. Am J Physiol Gastrointest Liver Physiol 301: G464-G474, 2011.
13. Hao ZM, Fan XB, Li S, Lv YF, Su HQ, Jiang HP and Li HH: Vaccination with platelet-derived growth factor B kinoids inhibits CCl(4)-induced hepatic fibrosis in mice. J Pharmacol Exp Ther 342: 835-842, 2012.
14. Takayama H, Miyake Y, Nouso K, Ikeda F, Shiraha H, Takaki A, Kobashi H and Yamamoto K: Serum levels of platelet-derived growth factor-BB and vascular endothelial growth factor as prognostic factors for patients with fulminant hepatic failure. J Gastroenterol Hepatol 26: 116-121, 2011.
15. van Dijk F, Olinga P, Poelstra K and Beljaars L: Targeted therapies in liver fibrosis: Combining the best parts of platelet-derived growth factor BB and interferon gamma. Front Med (Lausanne) 2: 72, 2015.
16. Hirota JA, Ask K, Farkas L, Smith JA, Ellis R, Rodriguez-Lecompte JC, Kolb M and Inman MD: In vivo role of platelet-derived growth factor-BB in airway smooth muscle proliferation in mouse lung. Am J Respir Cell Mol Biol 45: 566-572, 2011.
17. Rovida E, Navari N, Caligiuri A, Dello Sbarba P and Marra F: ERK5 differentially regulates PDGF-induced proliferation and migration of hepatic stellate cells. J Hepatol 48: 107-115, 2008.
18. Gressner AM and Weiskirchen R: Modern pathogenetic concepts of liver fibrosis suggest stellate cells and TGF-beta as major players and therapeutic targets. J Cell Mol Med 10: 76-99, 2006.
19. Patsenker E, Popov Y, Wiesner M, Goodman SL and Schuppan D: Pharmacological inhibition of the vitronectin receptor abrogates PDGF-BB-induced hepatic stellate cell migration and activation in vitro. J Hepatol 46: 878-887, 2007.
20. Lin X, Kong LN, Huang C, Ma TT, Meng XM, He Y, Wang QQ and Li J: Hesperetin derivative-7 inhibits PDGF-BB-induced hepatic stellate cell activation and proliferation by targeting Wnt/β-catenin pathway. Int Immunopharmacol 25: 311-320, 2015.
21. Fang L, Zhan S, Huang C, Cheng X, Lv X, Si H and Li J: TRPM7 channel regulates PDGF-BB-induced proliferation of hepatic stellate cells via PI3K and ERK pathways. Toxicol Appl Pharmacol 272: 713-725, 2013.
22. Shin HW, Park SY, Lee KB, Shin E, Nam SW, Lee JY and Jang JJ: Transcriptional profiling and Wnt signaling activation in proliferation of human hepatic stellate cells induced by PDGF-BB. Korean J Hepatol 15: 486-495, 2009.
23. Chen SW, Chen YX, Zhang XR, Qian H, Chen WZ and Xie WF: Targeted inhibition of platelet-derived growth factor receptor-beta subunit in hepatic stellate cells ameliorates hepatic fibrosis in rats. Gene Ther 15: 1424-1435, 2008.
24. Zeng Y, Liu H, Kang K, Wang Z, Hui G, Zhang X, Zhong J, Peng W, Ramchandran R, Raj JU and Gou D: Hypoxia inducible factor-1 mediates expression of miR-322: Potential role in proliferation and migration of pulmonary arterial smooth muscle cells. Sci Rep 5: 12098, 2015.
25. Liu LM, Zhang JX, Wang XP, Guo HX, Deng H and Luo J: Pim-3 protects against hepatic failure in D-galactosamine (D-GalN)-sensitized rats. Eur J Clin Invest 40: 127-138, 2010.
26. Maruyama H, Higuchi N, Nishikawa Y, Kameda S, Iino N, Kazama JJ, Takahashi N, Sugawa M, Hanawa H, Tada N, et al: High-level expression of naked DNA delivered to rat liver via tail vein injection. J Gene Med 4: 333-341, 2002.
27. Sayed RH, Khalil WK, Salem HA, Kenawy SA and El-Sayeh BM: Sulforaphane increases the survival rate in rats with fulminant hepatic failure induced by D-galactosamine and lipopolysaccharide. Nutr Res 34: 982-989, 2014.
28. Kara S, Gencer B, Karaca T, Tufan HA, Arikan S, Ersan I, Karaboga I and Hanci V: Protective effect of hesperetin and naringenin against apoptosis in ischemia/reperfusion-induced retinal injury in rats. Sci World J 2014: 797824, 2014.
29. Xiong Q, Hase K, Tezuka Y, Namba T and Kadota S: Acteoside inhibits apoptosis in D-galactosamine and lipopolysaccharide-induced liver injury. Life Sci 65: 421-430, 1999.
30. Kanno S, Ishikawa M, Takayanagi M, Takayanagi Y and Sasaki K: Characterization of hydrogen peroxide-induced apoptosis in mouse primary cultured hepatocytes. Biol Pharm Bull 23: 37-42, 2000.
31. Ogasawara J, Watanabe-Fukunaga R, Adachi M, Matsuzawa A, Kasugai T, Kitamura Y, Itoh N, Suda T and Nagata S: Lethal effect of the anti-Fas antibody in mice. Nature 364: 806-809, 1993.
32. Tanoi T, Tamura T, Sano N, Nakayama K, Fukunaga K, Zheng YW, Akhter A, Sakurai Y, Hayashi Y, Harashima H and Ohkohchi N: Protecting liver sinusoidal endothelial cells suppresses apoptosis in acute liver damage. Hepatol Res 46: 697-706, 2016.
33. Gao G, Yu Z, Yan J, Li J, Shen S, Jia B, Guan K, Gao X and Kan Q: Lowering blood ammonia prevents hepatocyte injury and apoptosis. Int J Clin Exp Med 8: 12347-12355, 2015.

34. Salabei JK, Cummins TD, Singh M, Jones SP, Bhatnagar A and Hill BG: PDGF-mediated autophagy regulates vascular smooth muscle cell phenotype and resistance to oxidative stress. Biochem J 451: 375-388, 2013.
35. Zheng L, Ishii Y, Tokunaga A, Hamashima T, Shen J, Zhao QL, Ishizawa S, Fujimori T, Nabeshima Y, Mori H, *et al*: Neuroprotective effects of PDGF against oxidative stress and the signaling pathway involved. J Neurosci Res 88: 1273-1284, 2010.
36. Zheng LS, Ishii Y, Zhao QL, Kondo T and Sasahara M: PDGF suppresses oxidative stress induced Ca^{2+} overload and calpain activation in neurons. Oxid Med Cell Longev 2013: 367206, 2013.
37. Krzystek-Korpacka M, Neubauer K and Matusiewicz M: Platelet-derived growth factor-BB reflects clinical, inflammatory and angiogenic disease activity and oxidative stress in inflammatory bowel disease. Clin Biochem 42: 1602-1609, 2009.
38. Urtasun R, Conde de la Rosa L and Nieto N: Oxidative and nitrosative stress and fibrogenic response. Clin Liver Dis 12: 769-790, 2008.
39. Saito Y, Hojo Y, Tanimoto T, Abe J and Berk BC: Protein kinase C-alpha and protein kinase C-epsilon are required for Grb2-associated binder-1 tyrosine phosphorylation in response to platelet-derived growth factor. J Biol Chem 277: 23216-23222, 2002.
40. Lindqvist A, Nilsson BO, Ekblad E and Hellstrand P: Platelet-derived growth factor receptors expressed in response to injury of differentiated vascular smooth muscle in vitro: Effects on Ca^{2+} and growth signals. Acta Physiol Scand 173: 175-184, 2001.
41. Cheng M, Park H, Engelmayr GC, Moretti M and Freed LE: Effects of regulatory factors on engineered cardiac tissue in vitro. Tissue Eng 13: 2709-2719, 2007.
42. Zhang L, Ma J, Shen T, Wang S, Ma C, Liu Y, Ran Y, Wang L, Liu L and Zhu D: Platelet-derived growth factor (PDGF) induces pulmonary vascular remodeling through 15-LO/15-HETE pathway under hypoxic condition. Cell Signal 24: 1931-1939, 2012.
43. Geiger A, Walker A and Nissen E: Human fibrocyte-derived exosomes accelerate wound healing in genetically diabetic mice. Biochem Biophys Res Commun 467: 303-309, 2015.
44. Chiang CH, Wu WW, Li HY, Chien Y, Sun CC, Peng CH, Lin AT, Huang CS, Lai YH, Chiou SH, *et al*: Enhanced antioxidant capacity of dental pulp-derived iPSC-differentiated hepatocytes and liver regeneration by injectable HGF-releasing hydrogel in fulminant hepatic failure. Cell Transplant 24: 541-559, 2015.
45. Vanlandewijck M, Lebouvier T, Andaloussi Mäe M, Nahar K, Hornemann S, Kenkel D, Cunha SI, Lennartsson J, Boss A, Heldin CH, *et al*: Functional characterization of germline mutations in PDGFB and PDGFRB in primary familial brain calcification. PloS One 10: e0143407, 2015.
46. Fjaer R, Brodtkorb E, Oye AM, Øye AM, Sheng Y, Vigeland MD, Kvistad KA, Backe PH and Selmer KK: Generalized epilepsy in a family with basal ganglia calcifications and mutations in SLC20A2 and CHRNB2. Eur J Med Genet 58: 624-628, 2015.
47. Zhang Q, Shi S, Liu Y, Uyanne J, Shi Y, Shi S and Le AD: Mesenchymal stem cells derived from human gingiva are capable of immunomodulatory functions and ameliorate inflammation-related tissue destruction in experimental colitis. J Immunol 183: 7787-7798, 2009.
48. Hwang GH, Jeon YJ, Han HJ, Park SH, Baek KM, Chang W, Kim JS, Kim LK, Lee YM and Lee S: Protective effect of butylated hydroxylanisole against hydrogen peroxide-induced apoptosis in primary cultured mouse hepatocytes. J Vet Sci 16: 17-23, 2015.
49. Ma X, Han S, Zhang W, Fan YJ, Liu MN, Liu AY and Liu BR: Protection of cultured human hepatocytes from hydrogen peroxi-deinduced apoptosis by relaxin-3. Mol Med Rep 11: 1228-1234, 2015.
50. Moniaux N, Song H, Darnaud M, Garbin K, Gigou M, Mitchell C, Samuel D, Jamot L, Amouyal P, Amouyal G, *et al*: Human hepatocarcinoma-intestine-pancreas/pancreatitis-associated protein cures fas-induced acute liver failure in mice by attenuating free-radical damage in injured livers. Hepatology 53: 618-627, 2011.
51. Ramsey HE, Da Silva CG, Longo CR, Csizmadia E, Studer P, Patel VI, Damrauer SM, Siracuse JJ, Daniel S and Ferran C: A20 protects mice from lethal liver ischemia/reperfusion injury by increasing peroxisome proliferator-activated receptor-alpha expression. Liver Transpl 15: 1613-1621, 2009.
52. Lou SM, Li YM, Wang KM, Cai WM and Weng HL: Expression of platelet-derived growth factor-BB in liver tissues of patients with chronic hepatitis B. World J Gastroenterol 10: 385-388, 2004.
53. Boulon S, Westman BJ, Hutten S, Boisvert FM and Lamond AI: The nucleolus under stress. Mol Cell 40: 216-227, 2010.
54. Russo A, Saide A, Smaldone S, Faraonio R and Russo G: Role of uL3 in multidrug resistance in p53-mutated lung cancer cells. Int J Mol Sci 18: E547, 2017.
55. Lv H, Qi Z, Wang S, Feng H, Deng X and Ci X: Asiatic acid exhibits anti-inflammatory and antioxidant activities against lipopolysaccharide and d-Galactosamine-induced fulminant hepatic failure. Front Immunol 8: 785, 2017.
56. Russo A, Saide A, Cagliani R, Cantile M, Botti G and Russo G: rpL3 promotes the apoptosis of p53 mutated lung cancer cells by down-regulating CBS and NFκB upon 5-FU treatment. Sci Rep 6: 38369, 2016.
57. Lawrence T: The nuclear factor NF-kappaB pathway in inflammation. Cold Spring Harb Perspect Biol 1: a001651, 2009.